

Annihilation of Dipolar Dark Matter to Photons

C. Arellano-Celiz^{1,3}, A. Avilez-López^{1,3}, J. E. Barradas-Guevara^{1,3}, O. Félix-Beltrán^{2,3a}

¹*Facultad de Ciencias Físico Matemáticas,
Benemérita Universidad Autónoma de Puebla,
Apdo. Postal 1152, Puebla, Pue., México.*

²*Facultad de Ciencias de la Electrónica,
Benemérita Universidad Autónoma de Puebla,
Apdo. Postal 542, C.P. 72570, Puebla, Pue., México.*

³*Centro Internacional de Física Fundamental (CUFFU), Puebla, Pue., C.P. 72570, México.*

(Dated: July 23, 2022)

Abstract

In this work we study the annihilation of fermionic dark matter, considering it as a neutral particle with non vanishing magnetic (M) and electric (D) dipole moments. Effective cross-section of the process $\chi\bar{\chi} \rightarrow \gamma\gamma$ is computed starting from a general form of coupling $\chi\bar{\chi}\gamma$ in the framework of an extension of the Standard Model. By taking into account annihilation of DM pairs into mono-energetic photons, we found that for small masses, $m_\chi \leq 10$ GeV, an electric dipole moment $\sim 10^{-16}$ e cm is required to satisfy the current residual density inferences. Additionally, in order to pin down models viable to describe the physics of dark matter at the early Universe we also constrain our model according to recent measurements of the temperature anisotropies of the cosmic background radiation, we report constraints to the electric and magnetic dipole moments for a range of masses within our model.

PACS numbers: 14.80.Bn, 12.60.Fr, 95.30.Cq, 95.35.+d

^a olga.felix@correo.buap.mx

I. INTRODUCTION

The enigma of dark matter (DM) is perhaps the most interesting problems in modern astrophysics, moreover that it has led to the incursion of elementary particle physics. The joint work of these two disciplines has as one of its main objectives to determine the nature and properties of DM, either through direct or indirect detection. This missing mass enigma emerged since was first figured out by F. Zwicky, and later V. Rubin measured the curves of galaxies and the masses of extragalactic systems [1, 2]. Nowadays, the evidences from galactic dynamics (rotation curves), galaxy clusters, structure formation, as well as the Big Bang’s nucleosynthesis and the cosmic background radiation, suggest that baryons do not suffice to explain observations; most of the non-relativistic missing matter prevailing in the Universe must be non-baryonic [3–6].

The non-baryonic nature of DM is a clear evidence that our understanding of the matter components of elementary particle physics, beautifully described by the Standard Model (SM) is incomplete. For this reason, theoretical physicists have considered new physics beyond the Standard Model (BSM) in order to accommodate (at least) a non-baryonic DM candidate [6, 7]. The only no weakly interacting particle within the SM is the neutrino, which has been shown to be inadequate to explain the features of the major DM fraction [8].

One of the most studied and well understood candidates emerging of BSM, are the weak interacting massive particles, commonly called as WIMPs. Examples of these are the neutralino [9] and the gravitino, but unfortunately they have not been detected yet. There are other compelling candidates of non-thermal origin such as the axion [10] and axion-like-particles [11], among others. In absence of the discovery of such particles it is worth exploring other possibilities. An alternative phenomenological researching line to explore the DM particle properties is an independent model. On this line, the restrictions for strongly interacting DM were considered in Ref. [12].

In addition, the DM self-interaction has been considered following the same approach in Refs. [13, 14]. Some people have studied whether DM could be charged [15] or if it might have a millicharge [16, 17]. Likewise, it has been considered among these phenomenological possibilities, that DM has an electric or/and magnetic dipole moment [18–23].

Annihilation of fermionic dark matter considering a DM particle with non vanishing magnetic (M) and electric (D) dipole moments (DDM) is the goal of this paper. By starting from a general form of coupling $\chi\bar{\chi}\gamma$ in a SM extension, the annihilation cross-section $\sigma_{ann} \equiv \sigma(\chi\bar{\chi} \rightarrow \gamma\gamma)$ is computed analytically.

The most stringent constraints on σ_{ann} are imposed in order to consistently predict measure-

ments in high energy experiments and astrophysical sources. On the other hand, cosmological observations provide weaker constraints to σ_{ann} since scattering processes involving DM affect the thermodynamics of the cosmic plasma due to injection energy and entropy to the cosmic plasma at the early Universe.

Nonetheless, the cosmological bounds are relevant since provide information about the features of DM in quite different regime. For example, it is well known that if DM couples to gauge bosons a resonance can be created which is amplified by low-velocity DM at late times in typical astrophysical environments and it is able to increase the cross-section by orders of magnitude, this effect is known as the Sommerfeld enhancement [24]. For that reason, even though constraints from high energy phenomena are stronger than those from cosmological observations, the latter are important to shape the features of DM at the early Universe. In this work our goal is to set constraints on DDM models focus on recent measurements of the temperature anisotropies of the cosmic background radiation and the current relic abundance.

In this work we consider, precisely, the annihilation of fermionic DM, considering it as a neutral particle with non vanishing magnetic (M) and electric (D) dipole moments. Effective cross-section of the process $\chi\bar{\chi} \rightarrow \gamma\gamma$ is made starting from a general form coupling $\chi\bar{\chi}\gamma$. We also constrain our model according to recent measurements of the temperature anisotropies of the cosmic background radiation.

Then, in the next section II we set up the theoretical framework behind the sort of DM considered here. In subsection II A, we introduce the effective Lagrangian describing the interaction between DDM and photons, as well as the calculation of the thermally averaged cross-section corresponding to the annihilation process $\langle\sigma_{ann}v_{rel}\rangle$. Afterwards, in section III we present our main results, which consist of constraints established over the magnetic and electric dipole moments, and the DM mass in order to satisfy some recent phenomenological constraints to $\langle\sigma_{ann}v_{rel}\rangle$ and the DM mass, by requiring the residual abundance and the cross-section to be consistent with measurements of the temperature anisotropies of the cosmic background radiation, subsections III A and III B. Finally, we give our conclusions in section IV.

II. THEORETICAL FRAMEWORK

Dark matter seems to be made of non-relativistic particles which mainly interact on a gravitational way with SM particles. Non-gravitational interactions might exist but they should be very weak in order to generate the observed large scale structures. There from, the DM coupling

to photons is assumed to be negligible [19]. However, although the DM particles are assumed as chargeless, they could be coupled to photons through radiative corrections in the electric (D) and magnetic (M) dipole moment [20]. Then, we assume DM as fermionic WIMPs particles endowed with a permanent electric and/or magnetic dipole moment [22].

Within the DDM framework $\chi\bar{\chi}$ pairs are able to annihilate into two photons through processes corresponding to the Feynman diagrams shown in Figure 1. There are other relevant annihilation processes such as $\chi\bar{\chi} \rightarrow \gamma Z^0$ and $\chi\bar{\chi} \rightarrow \gamma H^0$. However in this work we assume that the $\gamma\gamma$ channel is the most relevant in the cosmological scenario [25].

According to [25], the spectrum of secondary photons produced by annihilation is homogeneous and has a cutoff at $E_\chi = m_\chi$ where as it barely depends on m_χ and takes the same form for any channel, therefore we can assume that photons are monochromatic.

Likewise any WIMP, DDM particles might be detected either through direct and indirect methods. In the former, WIMPs would be detected by measuring a nuclear recoil produced in their on elastic collision with the detector nuclei as target in laboratory frame [18–20]. Examples of these experiments are CRESST [26, 27], XENON [28, 29], CDMS [30, 31], DAMA [32–34] and COGENT [35–37]. Besides, indirect methods allow us to detect a WIMP through the observation of secondary products emitted due to annihilation of $\chi\bar{\chi}$ pairs across the galactic halo or inside the Sun and the Earth, where they could have been gravitationally trapped. In this annihilation some kind of radiation would be emitted, such as: high energy photons (gamma rays), neutrinos, electron-positron and proton-antiproton pairs, among others. An example of these one is HAWC (High Altitude Water Cherenkov) [38].

On the other hand, possible signatures of DDM could arise in some cosmological grounds. Firstly, like any other WIMP, the cosmic relic abundance due to these DDM particles would have been formed owing to non-equilibrium thermal decoupling when the pair-annihilation rate dropped below the expansion rate of the Universe. That is, when the temperature of the cosmic plasma laid well below m_χ , DM particles are relativistic and the pair-annihilation of occurred in equilibrium. As the temperature drops below m_χ the species become non-relativistic and the particle number density starts to decrease tracking for a while the equilibrium behavior. At some point annihilations become fairly unlikely due to the cosmic expansion and the DM species goes out of equilibrium and freezes in Ref. [39]. This out-of equilibrium process leaves behind a DM cold relic that barely interacts with itself or any other particle except gravitationally [40].

For such a thermal particle with a weak-scale mass that annihilates through the s -channel, the relative density corresponding to its relic abundance can be inferred from different cosmological ob-

servations [6, 39, 41]. In particular, it is well known that the peak-structure of the CMB anisotropies is sensitive to the total amount of DM in the Universe at the time of recombination [42]. Therefore, in accordance with the recent precise measurements of these temperature anisotropies made by Planck the required total amount of cold DM at that epoch must be $\Omega_{cdm}h^2 = 0.112 \pm 0.0012$ [41]. Besides, this relative density can be computed through the asymptotic Boltzmann equation governing the thermodynamics of massive DM species during annihilation at the early Universe. In this process, as the more efficient is the annihilation process -for larger $\langle\sigma_{ann}v_{rel}\rangle$ - the smaller would be the left-over of DM after decoupling. Thus, this residual quantity is closely related to the thermally-averaged cross-section and bounds to the relative density give rise to constraints on the cross-section via the following relation [39, 43]

$$\Omega_{cdm}h^2 \approx \frac{3 \times 10^{-26} \text{cm}^3/\text{s}}{\langle\sigma_{ann}v_{rel}\rangle}, \quad (1)$$

with v_{rel} being the relative velocity.

In this way, the energy density of residual DDM particles is fixed by $\sigma_{ann}v_{rel}$. Note that the previous equation is in agreement with the description above smaller effective annihilation sections correspond to much higher residual densities. It is worth mentioning that, the value of $\Omega_{cdm}h^2$ shown above is an upper bound for the energy density of the DM relic. In a more realistic scenario, more than one DM species should be considered and therefore their overall energy density must not overpass such value.

In addition, annihilation of DDM have another effect of energy and entropy injection to the cosmic plasma nearby the recombination epoch since it ionizes the gas and results in an effective increase in the free electron fraction resulting in modification to the structure of the CMB spectrum [39, 44].

On the other hand, beyond the cosmological scenario, gamma rays provide a valuable piece of astronomical evidence for studying DM annihilation at local scales, since these photons are not deflected by intermediate magnetic fields between the source and the Earth, therefore the line of sight points towards the target where they are created. This allows us to look for gamma-ray signatures not only in our neighborhood of the galaxy, but also in distant objects such as satellite galaxies, the Milky Way, or even clusters of galaxies. Another advantage of the use of gamma-rays is that, in the local Universe, they do not suffer attenuation and, therefore, they retain the spectral information unchanged on Earth [45]. These advantageous features of gamma rays make the HAWC observatory appealing for studying observational signatures of DM candidates in general and specifically DDM.

Although HAWC is sensitive to photons from 100 GeV to 100 TeV, it has a maximum sensitivity in the range of 10 to 20 TeV, which makes it sensitive to diverse searches for DM annihilation, including extended sources, emission diffuse of gamma-rays, and the gamma rays emission coming of sub-halos of non-luminous DM. A subset of these sources includes dwarf galaxies, galaxy M31, the Virgo cluster and the galactic center. Likewise, the response of HAWC to gamma rays from these sources has been simulated in several channels of well-motivated DM annihilation (bb , tt , $\tau\tau$, W^+W^-) [46]. By now, this task is out of the scope of this work, nevertheless we plan to resume it in future works.

A. The effective Lagrangian for coupling

The effective Lagrangian for the coupling of a Dirac fermion with magnetic and electric dipole moment with the electromagnetic field is [22]

$$\mathcal{L}_{\gamma\chi} = -\frac{i}{2}\bar{\chi}\sigma_{\mu\nu}(M + D\gamma^5)\chi F^{\mu\nu}, \quad (2)$$

where χ denotes DDM field, $F^{\mu\nu}$ is the electromagnetic tensor, and the coupling form is given as $\sigma_{\mu\nu}(M + D\gamma^5)$, where D and M are the electrical and magnetic dipole moments respectively, both with units e cm.

For low energies such that γ -energy and DDM mass relation E_γ/m_χ , the photon is blind for $M - D$ difference. In Equation (2), $\chi\bar{\chi}$ pairs in the galactic halo or contained in any region of the Universe with high densities (centers of galaxies, clusters of galaxies), can annihilate directly to γX , where $X = \gamma, Z, H$ (H a Higgs boson). In this work we assume that the annihilation of DDM particles is towards two photons through the diagrams shown in Figure 1. Annihilations take place mainly through s -waves, so $\sigma_{ann}v_{rel}$ is almost independent of the speed and therefore independent of the temperature [40].

B. Effective cross-section of the annihilation process: $\chi\bar{\chi} \rightarrow \gamma\gamma$

We consider the annihilation process $\chi\bar{\chi} \rightarrow \gamma\gamma$ with the same DDM particle as the propagator. cross-section is computed in the frame of center of mass (CM). For this process one have two contributions at low order (see Figure 1). Hence, the amplitude of DDM annihilation is $\mathcal{M} = \mathcal{M}_1 + \mathcal{M}_2$, with $\mathcal{M}_{1,2}$ given as

$$\mathcal{M}_1 = -k_{2\nu}k_{1\mu}\epsilon_\rho^*(k_2)\epsilon_\lambda^*(k_1) \left[\bar{u}(p_2)\sigma^{\nu\rho}(M + D\gamma^5) \right] \frac{(q_1^2 + m_\chi^2)}{q_1^2 - m_\chi^2} \left[\sigma^{\mu\lambda}(M + D\gamma^5)u(p_1) \right], \quad (3)$$

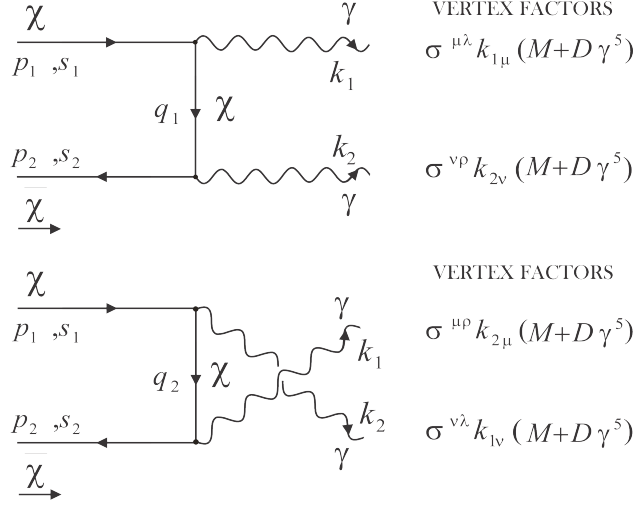


FIG. 1. Feynman diagrams for $\chi\bar{\chi} \rightarrow \gamma\gamma$.

$$\mathcal{M}_2 = -k_{1\nu} k_{2\mu} \epsilon_\lambda^*(k_1) \epsilon_\rho^*(k_2) \left[\bar{u}(p_2) \sigma^{\nu\lambda} (M + D\gamma^5) \right] \frac{(\not{q}_2 + m_\chi)}{q_2^2 - m_\chi^2} \left[\sigma^{\mu\rho} (M + D\gamma^5) u(p_1) \right]. \quad (4)$$

So, the total amplitude \mathcal{M} is

$$\begin{aligned} \mathcal{M} = & -\epsilon_\rho^*(k_2) \epsilon_\lambda^*(k_1) \bar{u}(p_2) \left[k_{2\nu} k_{1\mu} \sigma^{\nu\rho} (M + D\gamma^5) \left(\frac{\not{q}_1 + m_\chi}{q_1^2 - m_\chi^2} \right) \sigma^{\mu\lambda} (M + D\gamma^5) \right. \\ & \left. + k_{1\nu} k_{2\mu} \sigma^{\nu\lambda} (M + D\gamma^5) \left(\frac{\not{q}_2 + m_\chi}{q_2^2 - m_\chi^2} \right) \sigma^{\mu\rho} (M + D\gamma^5) \right] u(p_1), \end{aligned} \quad (5)$$

where k_1, k_2 and p_1, p_2 are the quadrimoments output and input respectively; q_1 and q_2 are the transferred quadrimoments, and m_χ is the DDM particle mass.

To compute $|\overline{\mathcal{M}}|^2$, we take into account that $p_1^2 = m_\chi^2$, $k_1^2 = 0$, and $k_2^2 = 0$ being that the resulting particles are photons. So, $|\overline{\mathcal{M}}|^2$ takes the expression

$$\begin{aligned} |\overline{\mathcal{M}}|^2 = & \frac{E_\chi^2}{E_\chi^2 - p^2 \cos^2 \theta} \left[16 (-m_\chi^4 + p^2 m_\chi^2 + E_\chi^4 + m_\chi^2 E_\chi^2 \right. \\ & - (2p^2 m_\chi^2 + 2p^2 E_\chi^2) \cos^2 \theta + p^4 \cos^4 \theta) (M^4 + D^4) \\ & + 32 (m_\chi^4 + 3p^2 m_\chi^2 - E_\chi^4 + 3m_\chi^2 E_\chi^2 + (2p^2 E_\chi^2 - 6p^2 m_\chi^2) \cos^2 \theta \\ & \left. - p^4 \cos^4 \theta) (M^2 D^2) \right], \end{aligned} \quad (6)$$

where p is the DDM moment and θ is the scattering angle.

Then, we derive the differential effective annihilation cross-section σ_{ann} , which reads as

$$\begin{aligned} \frac{d\sigma_{ann}}{d\Omega} = & \frac{1}{64\pi^2} \frac{E_\chi}{(2E_\chi)^2 p} \frac{E_\chi^2}{E_\chi^2 - p^2 \cos^2 \theta} \\ & \times [16(-m_\chi^4 + p^2 m_\chi^2 + E_\chi^4 + m_\chi^2 E_\chi^2 - (2p^2 m_\chi^2 + 2p^2 E_\chi^2) \cos^2 \theta + p^4 \cos^4 \theta)(M^4 + D^4) \\ & + 32(m_\chi^4 + 3p^2 m_\chi^2 - E_\chi^4 + 3m_\chi^2 E_\chi^2 + (2p^2 E_\chi^2 - 6p^2 m_\chi^2) \cos^2 \theta - p^4 \cos^4 \theta)(M^2 D^2)], \end{aligned} \quad (7)$$

where we use the Equation (6), as well as $|\mathbf{p}_1| = p$, $|\mathbf{p}_3| = E_\chi$, $E_1 = E_2 = E_\chi = \sqrt{p^2 + m_\chi^2}$, $|v_1 - v_2| = v_{rel} = \frac{2p}{E_\chi}$.

We need to compute $\langle \sigma_{ann} v_{rel} \rangle$ so that, using the method given by J. D. Wells in Ref. [47], we express (7) in terms of Mandelstam variables (s, t)

$$\begin{aligned} \frac{d\sigma_{ann}}{d\Omega} = & \frac{1}{128\pi^2} \frac{\sqrt{1-v_{cm}^2}}{m_\chi v_{cm} \sqrt{s}} \times \\ & \times \left[\frac{4(D^4 + M^4)m_\chi^4(s^2 + 10st + 6t^2) - 4tm_\chi^2(s+t)^2 + m_\chi^8 + t^2(s+t)^2}{(m_\chi^2 - t)(-m_\chi^2 + s + t)} \right. \\ & \left. + \frac{8D^2 M^2(-3m_\chi^4(s^2 + 2st - 2t^2) + 4tm_\chi^2(s^2 - t^2) + 4m_\chi^8(s-t) + m_\chi^8 + t^2(s+t)^2)}{(t - m_\chi^2)(-m_\chi^2 + s + t)} \right], \end{aligned} \quad (8)$$

where $|\mathbf{p}_1| = \frac{m_\chi v_{cm}}{\sqrt{1-v_{cm}^2}}$, $|\mathbf{p}_3| = \frac{\sqrt{s}}{2}$, $(E_1 + E_2)^2 = s$, $v_{cm} = \frac{v_{rel}}{2}$. Finally, in order to get the average of the thermal distribution of the WIMPs we need to compute $\langle \sigma_{ann} v_{rel} \rangle$ overall the phase-space variables. In that way, we get $\langle \sigma_{ann} v_{rel} \rangle$ needed to carry out further thermal analysis such as computing the residual abundance.

Since DM mean velocity is almost vanishing -hence the velocity dispersion-, we must work within the non-relativistic limit. Then, starting of Equation (8)-where it is possible to use the method described in Ref. [47], $\langle \sigma_{ann} v_{rel} \rangle$ is given as

$$\begin{aligned} \langle \sigma_{ann} v_{rel} \rangle = & \tilde{c}_0 m_{GeV}^2 \left[6(M_{16}^4 + 6M_{16}^2 D_{16}^2 + D_{16}^4) \right. \\ & \left. + (3M_{16}^4 + 2M_{16}^2 D_{16}^2 + 3D_{16}^4) \langle v_{rel}^2 \rangle \right] \text{cm}^3 \text{s}^{-1}, \end{aligned} \quad (9)$$

where $\tilde{c}_0 = 1.71423 \times 10^{-30}$, $m_{GeV} = \frac{m_\chi}{\text{GeV}}$, and both the magnetic and electric dipole moments have been normalized to be dimensionless: $D, M \rightarrow D_{16} = D/10^{-16}$, $M_{16} = M/10^{-16}$. On the other hand, using the relation $\langle \sigma_{ann} v_{rel} \rangle \approx a_{rel} + b_{rel} \langle v_{rel}^2 \rangle = a_{rel} + \frac{6b_{rel}}{x}$ given in [48], $\langle v_{rel}^2 \rangle = \frac{6}{x}$. Let us now to rewrite the predicted $\langle \sigma_{ann} v_{rel} \rangle$ in (9) as

$$\langle \sigma_{ann} v_{rel} \rangle = \tilde{c}_0 m_{GeV}^2 M_{16}^4 H(f), \quad (10)$$

where $x = \frac{m_\chi}{T}$ is the decoupling energy (T is temperature), which in non-relativistic limit $x \gg 1$ (or $T \ll m_\chi$), the dimensionless parameter $f \equiv \frac{D_{16}}{M_{16}}$ (which corresponds to the ratio of electric to

magnetic dipole moments respectively), and the dimensionless function $H(f, x)$:

$$H(f, x) = 6(1 + 6f^2 + f^4) + \frac{6}{x}(3 + 2f^2 + 3f^4). \quad (11)$$

We set x to the magical number $x = \frac{m_\chi}{T} \sim 22$, which is its typical value for WIMPS [49]. In this way, the theoretical parameter-set we shall use onward is $\{m_\chi, M_{16}, f\}$.

Notice that $\langle \sigma_{ann} v_{rel} \rangle$ increases either if m_χ and M_{16} do it, which implies that if m_χ or M_{16} increase, $\chi\bar{\chi}$ pairs annihilate more efficiently. Since the $H(f, x)$ factor is order one, the m_χ and the M_{16} just do control the order of magnitude of $\langle \sigma_{ann} v_{rel} \rangle$.

III. CONSTRAINTS ON THE DDM PARAMETERS SPACE ACCORDING TO PLANCK

In this section we determine a parameter-subspace of DDM models that is consistent with some cosmological constraints derived from Planck measurements of the temperature anisotropies of the cosmic background radiation. Firstly, in subsection III A, we consider phenomenological constraints in the $f_e \langle \sigma_{ann} v_{rel} \rangle - m_\chi$ plane (f_e a non perfect absorption efficiency is assumed) derived by Masi et al. [50] and by Kawasaki et al. [51], in order to infer the corresponding implications within our specific model and derive the allowed region of parameter space accordingly. The resulting bounds on the parameters will be taken as a prior assumption in our further statistical analysis carried out in the next section. Secondly, in III B we determine the projected posterior probability distribution (PPD) for m_χ , such that our prediction of the relative density of the cold DM relic $\Omega_{cdm} h^2$ is consistent with the most recent measurements according to Planck [41]. For that purpose, we sample the DDM parameter space using a grid-mesh in the three dimensional for it in order to compute the goodness-of-fit estimator χ^2 associated to the previously mentioned data-set.

A. Constraints from measurements of the Temperature Anisotropies of the CMB by Planck

In section II we have already explained how some observable signatures of DDM might appear in the features of the CMB. On one hand, let us recall that the overall DM abundance at recombination strongly determines the shape of the anisotropies of the CMB. On the other hand, DM annihilation injects energy to the electron-photon gas during such epoch, and consequently, the location and shape of the peaks of the CMB spectrum provide information about the magnitude of the annihilation cross-section and the mass of the DM particle [39].

Firstly, let us describe the phenomenological constraints considered here. In [50], bounds in the $f_e \langle \sigma_{ann} v_{rel} \rangle - m_\chi$ plane are derived and these are based on preliminary Planck results which are compatible with a s -wave annihilation cross-section around $10^{-23} \text{ cm}^3 \text{ s}^{-1}$ for $\sim \text{TeV}$ DM, in their analysis it is assumed an imperfect absorption efficiency $f_e \sim 0.2$ [52]. In despite of being preliminary, such constraints are consistent with posterior bounds reported in [51] inferred from Planck 2015. In that work, the effects of energy injection to the background plasma due to annihilations occurring at higher red-shift are simulated by using the methods established in [53]. As pointed out by the authors, CMB inferences have some advantages over cosmic ray ones, namely, CMB constraints do not depend on the DM distribution inside galaxies, which represents a source of systematic errors in cosmic ray experiments.

Now, let us analyze how constraints from CMB-Planck reduce the domain of the specific functional form of $\langle \sigma_{ann} v_{rel} \rangle$ computed in II B. Within the $f_e \langle \sigma_{ann} v_{rel} \rangle - m_\chi$ plane, the region laying below the dark-blue solid line in Figure 2 corresponds to the allowed models by the mentioned data-set. In there, the theoretical model proposed, gray dashed lines, show the $f_e \langle \sigma_{ann} v_{rel} \rangle$ as function of m_χ for $M_{16} = 0.117, 0.250, 0.670, 10.0$ and $f = 1$. For a model with a given M_{16} there exists a upper bound m_{up} , that is, particles with masses above m_{up} are excluded by CMB-Planck. The solid light-blue line in the same plane represents the WMAP5 constraint [54]. Notice that the upper bound for the mass from this data-set is weaker by more than one order of magnitude in comparison to the one corresponding to Planck.

Figure 2 also shows the lower limit for $\langle \sigma_{ann} v_{rel} \rangle$ in order not to overpass the observed relic of DM in the Universe, purple solid line. This bound on the cross-section gives rise to a lower bound m_{low} on m_χ for models within the allowed region (dark blue in Figure 2).

For a given dashed line associated to a single value of the dipole moment, only those values of m_χ for which the bit of line falling inside the blue region are allowed simultaneously by Planck and the relic abundance measurement. As it can be noticed for the $f = 1$ case in Figure 2, there is a cutoff ($M_{16}^* \sim 0.44$ for $f = 1$) above which DDM models are excluded. For dipole moments within this allowed threshold, the relic abundance bound provides a lower bound m_{low} satisfying the following relation (in general for any value of f),

$$\langle \sigma_{ann} v_{rel} \rangle_{relic} = \langle \sigma_{ann} v_{rel} \rangle^{th}(m_{low}, M_{16}, f) \quad (12)$$

$$2.5 \times 10^{-25} = \tilde{c}_0 \left(\frac{m_{low}}{\text{GeV}} \right)^2 M_{16}^4 H(f), \quad (13)$$

which leads to

$$\frac{m_{low}}{\text{GeV}} = \left(\frac{1.95 \times 10^{-15}}{M_{16}} \right)^2 \left(\frac{1}{H(f)} \right)^{1/2}. \quad (14)$$

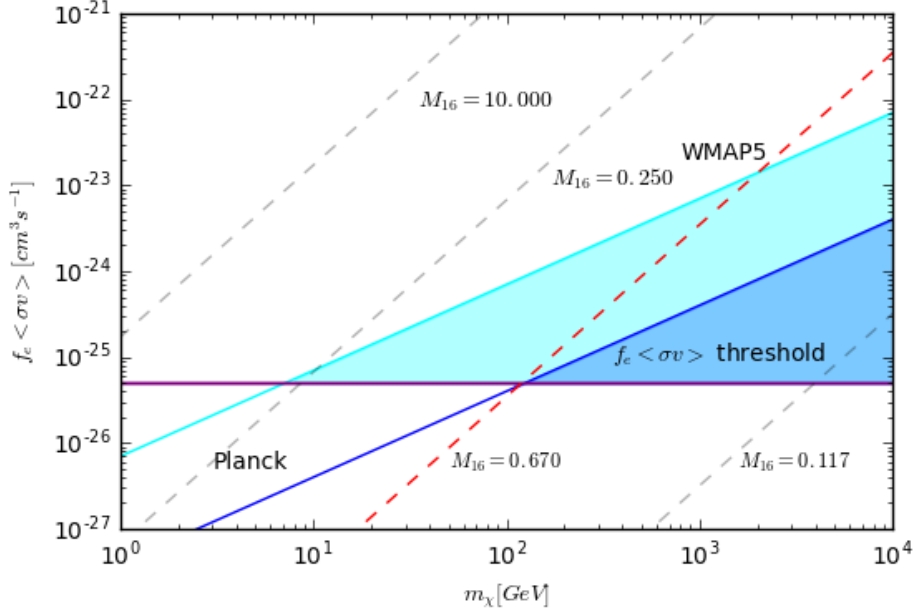


FIG. 2. Solid lines delimit regions of exclusion in the $f_e \langle \sigma_{ann} v_{rel} \rangle - m_\chi$ plane of WIMPs annihilating to photons according to CMB measurements. Dashed lines correspond to theoretical predictions within the DDM model for $f = 1$ and $M_{16} = 0.117, 0.250, 0.670, 10.0$.

Constraints from CMB measurements can be fitted by the following functional form:

$$f_e \langle \sigma_{ann} v_{rel} \rangle^{Planck} = (4 \times 10^{-28} \text{cm}^3 \text{s}^{-1}) m_{GeV}. \quad (15)$$

In a similar way as the relic abundance bound provides a lower bound m_{low} , the CMB-Planck constraint provides an upper bound for the DM particle mass m_χ within models with $M_{16} < M_{16}^*$, which satisfies $\sigma_P(m_{up}) = f_e \langle \sigma_{ann} v_{rel} \rangle^{th}(m_{up}, M_{16}, f)$.

This one implies that

$$\frac{m_{up}}{GeV} = \left(\frac{5.84}{M_{16}} \right)^4 \frac{1}{H(f)}. \quad (16)$$

In addition, for the more general case in which f is a free parameter, the top and bottom panels in Figure 3 illustrate the level-contours for functions $m_{up}(M_{16}, f)$, and $m_{low}(M_{16}, f)$ respectively, corresponding to the upper and lower bounds for models with different magnitudes of electric and magnetic dipole moments. In Figure 3, it is illustrated how both bounds for two chosen models can be determined. Both of them are representative, the first one (orange label) with $M_{16} = 0.5$ and $f = 1$ has equal electric and magnetic dipole moment close to the cutoff value M_{16}^* , while for the second model (purple label) a larger M_{16} is permitted as long as the $M_{16} - D_{16}$ ratio is reduced. For

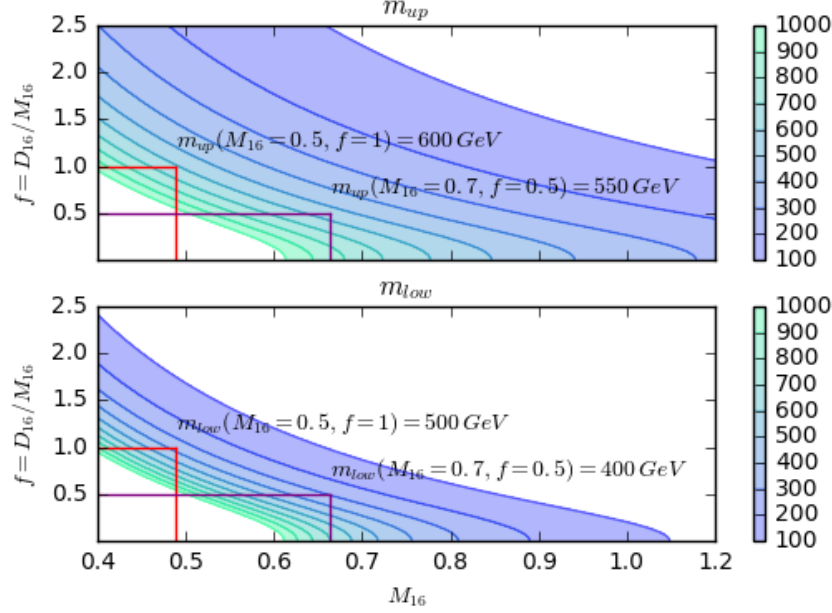


FIG. 3. Level-contours for $m_{up}(M_{16}, f)$ (top) and $m_{low}(M_{16}, f)$ (bottom). Each solid line corresponds to the upper and lower limits of DDM mass respectively for a variety of models with different values of dipole electric and magnetic moments according to Planck.

both models the allowed mass ranges lay around 400 – 600 GeV. It is clear from these figure, that f parameter notably relaxes the constraint on $M_{16} - m_\chi$ plane as expected. When $f = 1$ once M_{16} is fixed, the cutoff for m_χ is uniquely determined. In contrast, when M_{16} is fixed while f is free to vary, a whole range of masses are allowed.

B. Bounds from The Relative Density of DM Relic

In this subsection we derive bounds on the dipole moments and the mass of DDM from requiring that the predicted cold relic of these particles to be in accordance to the latest measurement by Planck. In the first part, we consider the whole three dimensional parameter space described at the beginning of this section. It is usual to fix the electric to magnetic dipole moment ratio to $f = 1$ under the argument that M_{16} and D_{16} arguments have the same order. However, even if $f \sim 1$ here we show that theoretical curves in the $\Omega_{cdm}h^2 - m_\chi$ plane are importantly sensitive to variations of f .

	Plik	CamSpec	Combinado
$\Omega_{cdm}h^2 \pm 1\sigma$	0.12 ± 0.0012	0.1197 ± 0.0012	0.1198 ± 0.0012

TABLE I. Cold DM relative density from Planck data-sets.

1. General Case: $D \neq M$

In this section we study the regions of the DDM space of parameters inside wide ranges of values of m_χ . Naturally, the purpose is to identify the regions of highest likelihood in accordance to the latest bounds to the DM relative density inferred from Planck. Before that, with the aim of getting an idea of the extent sensitivity of $\Omega_{cdm}h^2$ to each of the theoretical parameters, we explore the predicted $\Omega_{cdm}h^2 - m_\chi$ curves for different models.

We generated Figure 4 which clearly illustrates the effect of varying the dipole moments parameters M_{16} and f over $\Omega_{cdm}h^2$ as function of the DM particle mass. More specifically, three classes of $\Omega_{cdm}h^2(m_\chi)$ curves are shown which have a common value of f (associated with a given color). Each class contains curves of a models host with values of M_{16} within a fixed range of order 1. For a fixed M_{16} , the effect of varying f is clear, as it increases the $\Omega_{cdm}h^2 - m_\chi$ curves shift to smaller m_χ .

As a consequence, the values of m_χ picked by the data for DDM with non vanishing electric dipole moment (for a given value of M_{16}) are smaller than for DM holding only magnetic dipole moment. In other words, light DDM particles holding electric dipole moment are able to annihilate at the same rate than heavier particles with $f = 0$. In addition, there exists an overlap of curves of different classes, which is an indicator of a possible degeneracy between the parameters. Now let us proceed to describe the procedure used to sample the DDM parameter space. We calculated the χ^2 statistical estimator corresponding to the most recent measurement of the cold DM relative density from Planck data-sets shown in the Table I. For this purpose, the corresponding theoretical prediction is related to the thermally averaged cross-section computed previously in 1. We can assume, as a fair approximation, a normal likelihood distribution for Ω_{cdm} considering a flat prior. Thus, based on the Bayes theorem the posterior probability of a model associated to a point in parameter space (m_χ, M_{16}, f) to describe a measurement of $\Omega_{cdm}h^2$ reads

$$P(\Omega_{cdm}^{(th)}|\Omega_{cdm}^{(ob)}) = e^{-\chi^2} \quad \text{where} \quad \chi^2(m_\chi, M, f) = \frac{\left(\Omega_{cdm}^{(th)}(m_\chi, M, f) - \Omega_{cdm}^{(ob)}\right)^2}{\sigma^2}$$

where σ is the observational error and $\Omega_{cdm}^{(ob)}$ is the best-fit central value of the Planck collaboration estimation. By computing numerically the χ^2 described below, we sampled the parameters space

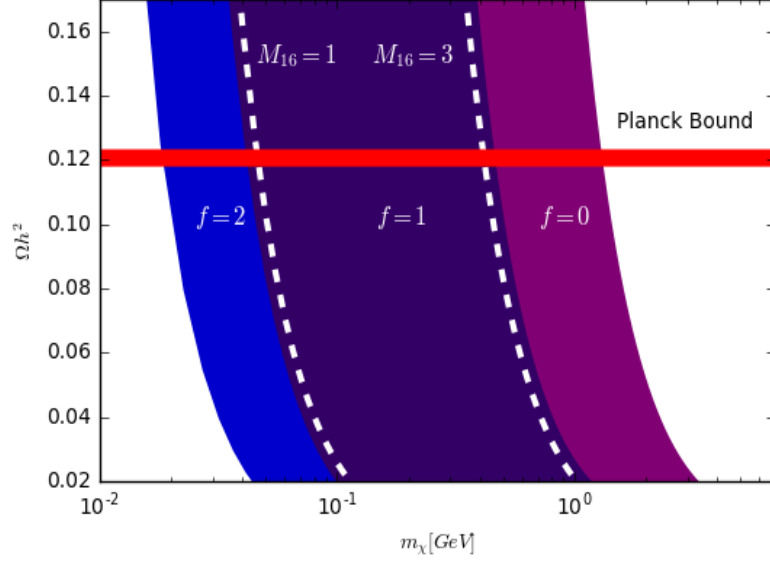


FIG. 4. Blue, purple and magenta regions correspond to the theoretically predicted regions of the DM relative density for $f = 2, 1, 0$ respectively. Within each region M_{16} runs between $[1, 3]$. Graph shows the residual abundance (1) for $D_{16} = 3$.

of the DDM model and set the bound found in section III A as a prior.

The main result of this part is presented in Figure 5. In there, various marginalized posterior distributions for the m_χ parameter are shown for fixed $M_{16} < M_{16}^*$ below the maximum value of the dipole moment consistent with CMB constraints found in III A and different values of f . Consistently with the analysis made at the beginning of this subsection, the estimation of m_χ shifts to lower values as f is raised.

2. Equal electric and magnetic dipole moments $f = 1$

Now let us consider, that $D_{16} = M_{16}$ under the assumption that both electrical and magnetic dipole moments are the same order of magnitude. Therefore, the annihilation effective cross-section expression by the relative thermally averaged speed for the process $\chi\bar{\chi} \rightarrow \gamma\gamma$ is:

$$\langle \sigma_{ann} v_{rel} \rangle = 48 \tilde{c}_0 m_{GeV}^2 D_{16}^4 \left[1 + \frac{1}{x} \right] \text{cm}^3 \text{s}^{-1}. \quad (17)$$

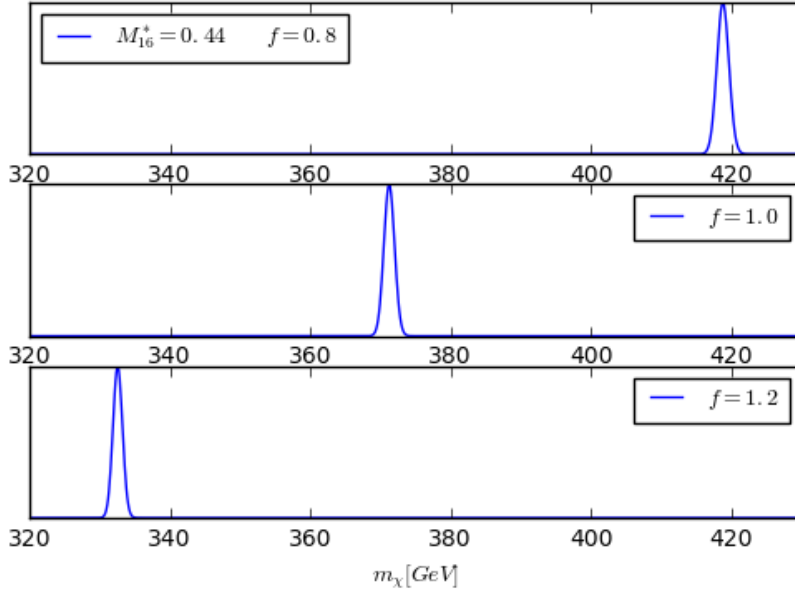


FIG. 5. 1D projection posterior distributions for the DM mass for the following values of the electric/magnetic dipole moments ratio $f = 0.8, 1.0, 1.2$ and magnetic dipole moment equal to the cutoff $M_{16}^* = 0.44$ established by CMB-Planck data.

We are taking into account the upper limit for dipole moments, $D_{16} = M_{16} \leq 3$, reported by K. Sigurdson et al. [22] and the decoupling energy for the WIMPs, $x \cong 22$. Note that $\langle \sigma_{ann} v_{rel} \rangle$ has the order of magnitude corresponding to the total annihilation cross-section for a generic WIMP, which is usually set as $\langle \sigma_{ann} v_{rel} \rangle_{D_{16}=3} \simeq 3 \times 10^{-26} \text{ cm}^3 \text{ s}^{-1}$ [55].

On the other hand, since the residual density of cold DM estimated by WMAP is [56], we can relate Equation (17) with (1) to obtain $\Omega_{cdm} h^2 \approx 0.11$. Then, if DDM particles are cold dark matter, it implies that the DDM particle mass density depends on the electrical dipole moment M_{16} and the mass m_χ . Therefore, for electrical dipole moments below e cm and masses it is always satisfied with the residual abundance given by WMAP (see Figure 2). In this particular case in which $f = 1$ is assumed, there is an upper bound for the dipole moment given by $M_{16}^* \sim 0.44$ implied by CMB measurements by Planck. Even though candidates with $M_{16} > M_{16}^*$ can be compatible with the relic abundance observations for a range of masses, they are excluded by the Planck-CMB measurements. Particle masses with dipole moment $M_{16} \sim M_{16}^*$ (tick purple line in Figure 6) are very restricted and lay in a narrow range around $m_\chi^* \sim 500 \text{ GeV}$ in order to be consistent with relic abundance observations. Although particles of this kind with masses $m_\chi < m_\chi^*$ are allowed by CMB measurements, their thermally averaged annihilation cross-section would be insufficient

Mass range m_χ [GeV]	Range of D [e cm]
$6 \leq m_\chi \leq 10$	$2.37 \times 10^{-16} \leq D \leq 3.0 \times 10^{-16}$
$10 \leq m_\chi \leq 100$	$7.5 \times 10^{-17} \leq D \leq 2.37 \times 10^{-16}$
$100 \leq m_\chi \leq 1000$	$2.38 \times 10^{-17} \leq D \leq 7.5 \times 10^{-17}$
$1000 \leq m_\chi \leq 10000$	$2.38 \times 10^{-18} \leq D \leq 2.38 \times 10^{-17}$
$10000 \leq m_\chi \leq 20000$	$5.3 \times 10^{-18} \leq D \leq 7.5 \times 10^{-18}$

TABLE II. Required DDM masses and range of values of electrical dipole moment that satisfies residual abundance $\Omega_{cdm} h^2 = 0.11$.

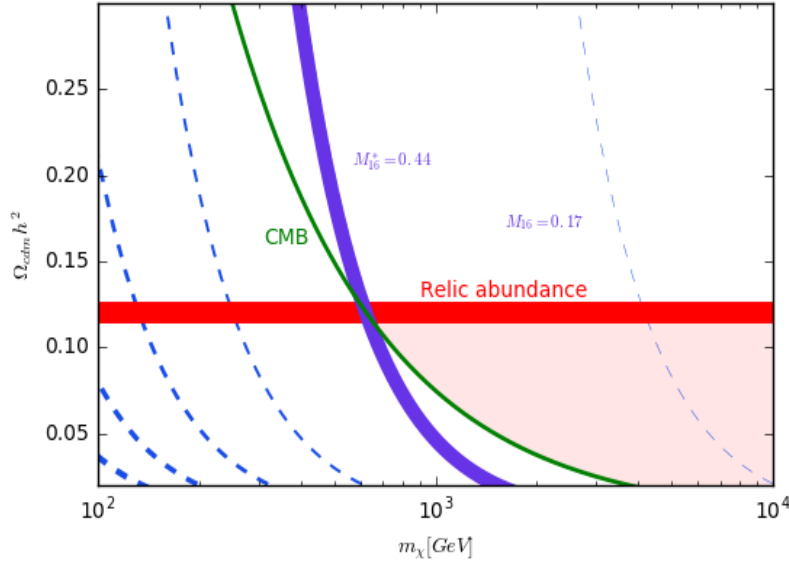


FIG. 6. The DM relative energy density. The red stripe shows the nowadays relative density of DM inferred from CMB measurements by Planck. Each purple line corresponds to the theoretical prediction of the relative density as a function of m_χ . Different dashed lines correspond to several values of the magnetic dipole moment assuming that $M_{16} = D_{16}$.

in order reduce the primeval DM abundance to give the DM relative density observed today. On the other hand, more massive candidates with the same value of M_{16} are excluded by the CMB observations. Notice that the allowed range of masses is very sensitive to variations of $M_{16} \gtrsim M_{16}^*$. A slight decrease in M_{16} (from M_{16}^* to $M_{16} = 0.17$) shifts the $\Omega_{cdm} h^2$ curve almost an order of

magnitude towards larger masses. Additionally, models within that range are able to consistently predict the relic abundance but only making up a fraction larger than the green line.

In conclusion, on this final combined analysis, by considering both the relic abundance and the CMB measurements, a host of models with low masses and large M_{16} are excluded. After considering the latter set, the first two rows in Table II are excluded.

IV. CONCLUSIONS

In this work we studied the DM annihilation, considering it as a neutral particle with non vanishing magnetic and/or electric moments. Therefore, we studied this candidate with $M \sim D$ laying below the upper bound of $3 \times 10^{-16} \text{ e cm}$ obtained in previous works [22]. The effective annihilation cross-section $\chi\bar{\chi} \rightarrow \gamma\gamma$ was analytically computed from first principles. In addition, we restricted the parameters space involved in the thermally averaged annihilation cross-section in order that the DDM model to be consistent with cosmological data, such as the relative density of the DM relic abundance and measurements of the temperature anisotropies of the cosmic background radiation. Then, we considered the model-independent constraint in the $f_e \langle \sigma_{ann} v_{rel} \rangle - m_\chi$ plane derived in [51], and one analyzed its implications over the DDM model parameter space. Firstly, by imposing these CMB bounds and fixing M_{16} , f values, there exists an upper bound for DDM particle mass, m_{up} . Moreover, in order to m_χ to be consistent with measurements of the DM relative density today a lower bound m_{low} is imposed. The resulting allowed mass range lies around 500 GeV. We also demonstrated that if f is taken as a free parameter (while remaining order one), then the allowed range of M_{16} , consistent with the CMB data-set, becomes pretty wide. As a second step, we analyzed the CMB constraint implications and the relic abundance measurement as well. By combining both priors, we found the upper cutoff $M_{16}^* = 0.44$ for the magnetic dipole moment (when $f \sim 1$). Afterwards, we estimated the projected posterior distributions for m_χ taken several f values, and by fixing the magnetic dipole moment M_{16} to a value below M_{16}^* in accordance to the CMB prior.

ACKNOWLEDGMENTS

This work has been partially supported by CONACYT-SNI (México).

- [1] F. Zwicky, *Helv. Phys. Acta* **6**, 110 (1933), [Gen. Rel. Grav.41,207(2009)].
- [2] V. C. Rubin, J. Burley, A. Kiasatpoor, B. Klock, G. Pease, E. Rutscheidt, and C. Smith, *Phys* **67**, 491 (1962).
- [3] P. J. E. Peebles, *Nat. Astron.* **1**, 0057 (2017), arXiv:1701.05837 [astro-ph.CO].
- [4] M. Roos, *Journal of Modern Physics* **3**, 1152 (2012).
- [5] L. Bergström, *Reports on Progress in Physics* **63**, 793 (2000).
- [6] G. Bertone, D. Hooper, and J. Silk, .
- [7] G. Jungman, M. Kamionkowski, and K. Griest, *Phys. Report* **267**, 195 (1996), arXiv:hep-ph/9506380 [hep-ph].
- [8] N. Fornengo, 36th COSPAR Scientific Assembly Beijing, China, July 16-23, 2006, *Adv. Space Res.* **41**, 2010 (2008), arXiv:astro-ph/0612786 [astro-ph].
- [9] G. Jungman, M. Kamionkowski, and K. Griest, *Phys. Rept.* **267**, 195 (1996), arXiv:hep-ph/9506380 [hep-ph].
- [10] M. S. Turner, BNL Workshop: Axions 1989:0001-38, *Phys. Rept.* **197**, 67 (1990).
- [11] L. Hui, J. P. Ostriker, S. Tremaine, and E. Witten, *Phys. Rev.* **D95**, 043541 (2017).
- [12] G. D. Starkman, A. Gould, R. Esmailzadeh, and S. Dimopoulos, *Phys. Rev. D* **41**, 3594 (1990).
- [13] E. D. Carlson, M. E. Machacek, and L. J. Hall, *The Astrophysical Journal* **398**, 43 (1992).
- [14] D. N. Spergel and P. J. Steinhardt, *Phys. Rev. Lett.* **84**, 3760 (2000).
- [15] A. Gould, B. T. Draine, R. W. Romani, and S. Nussinov, *Phys. Lett.* **B238**, 337 (1990).
- [16] S. Davidson, S. Hannestad, and G. Raffelt, *JHEP* **05**, 003 (2000), arXiv:hep-ph/0001179 [hep-ph].
- [17] S. L. Dubovsky, D. S. Gorbunov, and G. I. Rubtsov, *JETP Lett.* **79**, 1 (2004), [*Pisma Zh. Eksp. Teor. Fiz.*79,3(2004)], arXiv:hep-ph/0311189 [hep-ph].
- [18] J. H. Heo, *Phys. Lett.* **B693**, 255 (2010), arXiv:0901.3815 [hep-ph].
- [19] J. H. Heo, *Phys. Lett.* **B702**, 205 (2011), arXiv:0902.2643 [hep-ph].
- [20] E. Masso, S. Mohanty, and S. Rao, *Phys. Rev.* **D80**, 036009 (2009), arXiv:0906.1979 [hep-ph].
- [21] S. Profumo and K. Sigurdson, *Phys. Rev.* **D75**, 023521 (2007), arXiv:astro-ph/0611129 [astro-ph].
- [22] K. Sigurdson, M. Doran, A. Kurylov, R. R. Caldwell, and M. Kamionkowski, *Phys. Rev. D* **70**, 083501 (2004).
- [23] V. Barger, W.-Y. Keung, and D. Marfatia, *Phys. Lett.* **B696**, 74 (2011).
- [24] M. Lattanzi and J. I. Silk, *Phys. Rev.* **D79**, 083523 (2009).
- [25] T. Bringmann and C. Weniger, *Phys. Dark Univ.* **1**, 194 (2012).

- [26] F. Petricca et al. (CRESST), in (TAUP 2017) Sudbury, Ontario, Canada, July 24-28, 2017 (2017) arXiv:1711.07692 [astro-ph.CO].
- [27] A. H. Abdelhameed et al. (CRESST), (2019), arXiv:1904.00498 [astro-ph.CO].
- [28] M. Alfonsi (XENON), 37th Int. Conf. on High Energy Phys. (ICHEP 2014): Valencia, Spain, July 2-9, 2014, Nucl. Part. Phys. Proc. **273-275**, 373 (2016).
- [29] R. Essig, T. Volansky, and T.-T. Yu, Phys. Rev. **D96**, 043017 (2017), arXiv:1703.00910 [hep-ph].
- [30] R. Agnese et al. (SuperCDMS), Phys. Rev. **D92**, 072003 (2015), arXiv:1504.05871 [hep-ex].
- [31] S. J. Witte and G. B. Gelmini, JCAP **1705**, 026 (2017), arXiv:1703.06892 [hep-ph].
- [32] R. Bernabei et al., in 18th Lomonosov Conf. on Elem. Part. Phys.: Moscow, Russia, August 24-30, 2017 (2019) pp. 318–327.
- [33] G. Adhikari et al. (COSINE-100, The Sogang Phenomenology Group), JCAP **1906**, 048 (2019), arXiv:1904.00128 [hep-ph].
- [34] S. Baum, K. Freese, and C. Kelso, Phys. Lett. **B789**, 262 (2019), arXiv:1804.01231 [astro-ph.CO].
- [35] C. E. Aalseth et al. (CoGeNT), Phys. Rev. **D88**, 012002 (2013), arXiv:1208.5737 [astro-ph.CO].
- [36] J. H. Davis, C. McCabe, and C. Boehm, JCAP **1408**, 014 (2014), arXiv:1405.0495 [hep-ph].
- [37] C. E. Aalseth et al. (CoGeNT), (2014), arXiv:1401.3295 [astro-ph.CO].
- [38] A. U. Abeysekara et al., Astropart. Phys. **50-52**, 26 (2013), arXiv:1306.5800 [astro-ph.HE].
- [39] E. W. Kolb and M. S. Turner, Front. Phys. **69**, 1 (1990).
- [40] L. Bergström, Reports on Progress in Physics **63**, 793 (2000).
- [41] N. Aghanim et al. (Planck), (2018), arXiv:1807.06209 [astro-ph.CO].
- [42] P. Anninos, Living Reviews in Relativity **1** (2001), 10.12942/lrr-2001-2.
- [43] N. Arkani-Hamed, D. P. Finkbeiner, T. R. Slatyer, and N. Weiner, Phys. Rev. D **79**, 015014 (2009).
- [44] N. Padmanabhan and D. P. Finkbeiner, Phys. Rev. D **72**, 023508 (2005).
- [45] S. Funk, Sackler Colloquium: Dark Matter Universe: On the Threshold of Discovery Irvine, (2013), 10.1073/pnas.1308728111, [Proc. Nat. Acad. Sci.112,2264(2015)], arXiv:1310.2695 [astro-ph.HE].
- [46] Abeysekara et al. (HAWC Collaboration), Phys. Rev. D **90**, 122002 (2014).
- [47] J. D. Wells, (1994), arXiv:hep-ph/9404219 [hep-ph].
- [48] M. Cannoni, Eur. Phys. J. **C76**, 137 (2016), arXiv:1506.07475 [hep-ph].
- [49] M. Drees, H. Imminiyaz, and M. Kakizaki, Phys. Rev. D **76**, 103524 (2007).
- [50] N. Masi, European Physical Journal Plus **130**, 69 (2015).
- [51] M. Kawasaki, K. Nakayama, and T. Sekiguchi, Phys. Lett. **B756**, 212 (2016).
- [52] M. S. Madhavacheril, N. Sehgal, and T. R. Slatyer, Phys. Rev. **D89**, 103508 (2014).
- [53] T. Kanzaki, M. Kawasaki, and K. Nakayama, Prog. Theor. Phys. **123**, 853 (2010).
- [54] T. Barreiro, O. Bertolami, and P. Torres, Phys. Rev. **D78**, 043530 (2008), arXiv:0805.0731 [astro-ph].
- [55] G. Steigman, B. Dasgupta, and J. F. Beacom, Phys. Rev. **D86**, 023506 (2012), arXiv:1204.3622 [hep-ph].

- [56] C. L. Bennett, D. Larson, J. L. Weiland, N. Jarosik, G. Hinshaw, N. Odegard, K. M. Smith, R. S. Hill, B. Gold, M. Halpern, E. Komatsu, M. R. Nolta, L. Page, D. N. Spergel, E. Wollack, J. Dunkley, A. Kogut, M. Limon, S. S. Meyer, G. S. Tucker, and E. L. Wright, *The Astrophysical Journal Supplement Series* **208**, 20 (2013).